UDC 629.439
DOI 10.17816/transsyst201843143-153

© V.A. Polyakov, N.M. Khachapuridze
Institute of Transport Systems and Technologies of Ukraine's National Academy of Sciences (Dnepr, Ukraine)

MAGNETICALLY LEVITATED TRAIN'S LONGITUDINAL MOTION (SIMULATION RESULTS)

Background: The no-stationary regimes of the magnetically levitated train's (MLT) motion were the object of research.

Aim: The purpose of the study is to evaluate its dynamic qualities and loading in such regimes.

Methods: The work was carried out by conducting a series of experiments with a computer model of train's dynamics.

Results: The simulation results reflect its motion in the modes of acceleration, passage of the tunnel, as well as service and emergency braking.

Conclusion: An analysis of these results made it possible to evaluate the dynamic properties of a train in various non-stationary motion modes and its loading in their process.

Keywords: magnetically levitated train, non-stationary regimes of motion, dynamic qualities, dynamic loading, computer experiment.

© В.А. Поляков, Н.М. Хачапуридзе
Институт транспортных систем и технологий Национальной академии наук Украины, Днепр, Украина

ПРОДОЛЬНОЕ ДВИЖЕНИЕ МАГНИТОЛЕВИТИРУЮЩЕГО ПОЕЗДА (РЕЗУЛЬТАТЫ МОДЕЛИРОВАНИЯ)

Обоснование: Объектом исследования были нестационарные режимы движения магнитолевитирующего поезда (MLT).

Цель: Целью исследования явилась оценка его динамические качества и нагруженности в таких режимах.

Методы: Работа была выполнена путем проведения серии экспериментов с компьютерной моделью динамики поезда.

Результаты: Результаты моделирования отражают его движение в режимах ускорения, прохождения туннеля, а также сервисного и экстренного торможения.

Received: 11.08.2018. Revised: 11.08.2018. Accepted: 01.10.2018.
Transportation Systems and Technology. 2018;4(3):143-153

doi: 10.17816/transsyst201843143-153

Выводы: Анализ этих результатов позволил оценить динамические свойства поезда в различных нестационарных режимах движения и его загруженность в их процессе.

Ключевые слова: магнитолевитирующий поезд, нестационарные режимы движения, динамические качества, динамическая нагруженность, компьютерный эксперимент.

INTRODUCTION

The magnetically levitated train (MLP) is a large, complex system, the elements of which are very diverse. It's main purpose is to transport passengers and cargo. Quality of transportation is the key criterion for assessing the consumer properties of a train.

The dynamics of the electromechanical subsystem determines the specified quality. Particularly critical are the non-stationary modes of its motion. They are restrictive and subject to priority research. Carrying out such research is the main task of the work.

THE MATERIAL AND RESULTS OF THE STUDY

The one-dimensional longitudinal motion of MLT is considered. The calculated scheme of its mechanical subsystem (MS) is adopted in the form of a solid body of mass m. It's motion is considered with respect to an inertial fixed Cartesian reference frame $OXYZ$. The Cartesian triadron $Cxyz$, axes of which are it's main central ones, is connected with this body. The change of body's position in time t is determined by Cartesian coordinate $x(t)$ of it's center of mass. The analytical connections on the body are not imposed. The MS's of MLT's configuration is described by one generalized coordinate:

$$\eta^1 = x\,. \tag{1}$$

The motion is considered in an electrodynamics' levitation state – after separation from the direction-controlling structures. In the process of motion, the body's mass m center's deviations from a stationary trajectory parallel to the curve of the axis of the path and symmetrically disposed concerning it's structures are considered to be absent. The following forces acts on the body [1–3]:

F_{Tx} – from the side of the linear synchronous motor (LSM) – the longitudinal component of the traction force; F_{ADx} – from the ambient air – longitudinal component of the aerodynamic force; F_{EDx} – on the side of the track suspension loops – component of electrodynamics' force; F_{Wx} – due to the presence of a longitudinal slope of the track – longitudinal component of train's weight.

Received: 11.08.2018. Revised: 11.08.2018. Accepted: 01.10.2018.

doi: 10.17816/transsyst201843143-153

The longitudinal translational motion of a MLT's MS is described by the equation of Newton's second law:

$$m \cdot \ddot{x} = F_{Tx} + F_{ADx} + F_{EDx} + F_{Wx}, \quad (2)$$

where $\ddot{x}$ – is the longitudinal component of the C point's acceleration.

The values of the quantities F_{Tx}, in the case under consideration, are determined [4–6] by the relations:

$$F_{Tx} = f_{x\lambda\chi} \cdot e^{\lambda} \cdot e^{\chi}; \; e^{\lambda} = e^{\chi} = 1;$$

$$f_{\lambda\chi} = l_{\lambda\chi} \cdot i^{\lambda} \cdot \mathrm{B}_{\lambda\chi} \; \forall \lambda \in [\overline{1,N}], \chi \in [\overline{1,2}], \quad (3)$$

where $f_{\lambda\chi}$ – force of interaction of fields of currents of the χ-it rectilinear element of the λ-mp loop of inductor of the motor and its armature; $l_{\lambda\chi}, i^{\lambda}, \mathrm{B}_{\lambda\chi}$ – the length of such an element, the current in it, and also the induction (conditionally homogeneous – within the element) of the magnetic field in which the element is located.

The values of the quantities F_{ADx} are estimated [7–9] in the following way:

$$F_{ADx} = -C_x \cdot q \cdot S; \; q = 0.5 \cdot \rho \cdot \dot{x}^{(2)}, \quad (4)$$

where C_x – is the dimensionless aerodynamic coefficient in the direction of Cx; S – characteristic cross-sectional area of the train in the same direction; ρ – ambient air density.

The values of the quantities F_{EDx} are approximated [10–12] by a polynomial of the form:

$$F_{EDx} = k_{\rho} \cdot \dot{x}^{\rho} \cdot e^{\rho}; \; e^{\rho} = 1 \; \forall \; \rho \in [\overline{1, n_r}], \quad (5)$$

in which $k_{\rho} \; \forall \rho \in [\overline{1, n_r}]$ – are obtained by regressing the experimental dependences $F_{EDx}(t)$ with the selected degree of the approximation polynomial n_r.

Finally, the change of the force values F_{Wx} is described by the expression:

$$F_{Wx} = m \cdot g \cdot \sin \varphi_{\kappa}, \quad (6)$$

where g – is the gravitational constant; φ_{κ} – the angle of the gradient of the profile of the way section, along which the train moves.

The mathematical model (2) describes the longitudinal one-dimensional motion of the MLT's MS under the influence of external disturbances, as well

Received: 11.08.2018. Revised: 11.08.2018. Accepted: 01.10.2018.

Transportation Systems and Technology. 2018;4(3):143-153
doi: 10.17816/transsyst201843143-153

as control from its LSM. This model was adopted as an algorithmic basis for constructing a relevant computer model of the same process of motion, which is an instrument for its study. The elements of the computer model are programmatically fixed within the input language of the Mathematica computer mathematics system and are divided into the calculation and graphical parts. The first of these parts, functionally, solves the direct problem of the dynamics of the system under study, and the second of the parts – converts the results of calculations into a graphic form. The study was carried out by conducting a series of experiments with this computer model. Their results, in each of the considered modes of motion, were the graphs of the functional dependencies on time of various quantities characterizing and generating this motion. The motion was studied in the following non-stationary regimes: increasing the speed (from the moment of transition to the state of electrodynamics' levitation to the steady speed of motion); passage through the tunnel; service and emergency braking. Some of the results of this study are presented and analyzed further.

The frequency of the voltage, that feeds the LSM's armature winding, is always automatically maintained [1] by the proportional of the MLT's speed. In addition to frequency, system's control can have an additional component that provides an increase in the smoothness of electromagnetic processes in the LSM and a mechanical component in the MS. As such a component, amplitude or phase control can be used. In the first of these cases, in the process of increasing the MLT's speed, the smoothness of the LSM's power supply is provided by increasing the voltage amplitude, which is applied to its armature winding, for example, according to the law

$$U_a(t) = U_a^* \cdot th(t \cdot k_{vd}), \qquad (7)$$

where U_a^* – is the limiting value of this amplitude; k_{vd} – coefficient, which determines the intensity of the voltage amplitude increasing.

In the case of the phase variant of controlling the train speed increase, the initial phase of the armature voltage can vary, for example, according to law

$$\theta_u(t) = \alpha_u \cdot [th(t \cdot k_{fd}) - 1], \qquad (8)$$

where α_u – is it's current phase; k_{fd} – coefficient, that determines the rate of initial phase changing.

Illustrative examples of the results of the investigation of the MLT's motion in the regime of increasing the speed are shown in Fig. 1–6. Fig. 1, 2 correspond to the control of only the frequency of the voltage; Fig. 3, 4 – amplitude-frequency

Received: 11.08.2018. Revised: 11.08.2018. Accepted: 01.10.2018.

doi: 10.17816/transsyst201843143-153

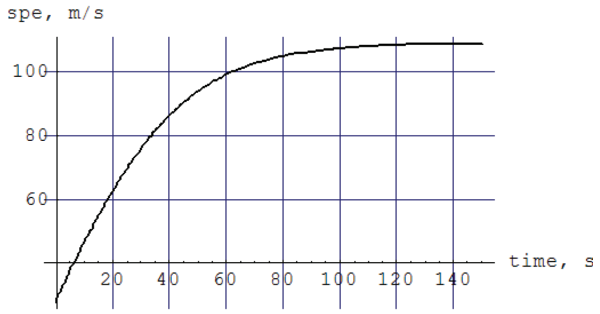

Fig. 1. The train's speed graph

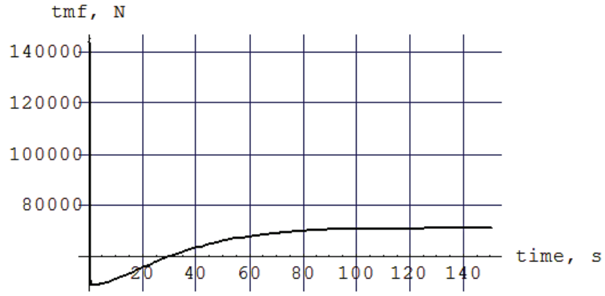

Fig. 2. The LSM's traction force graph

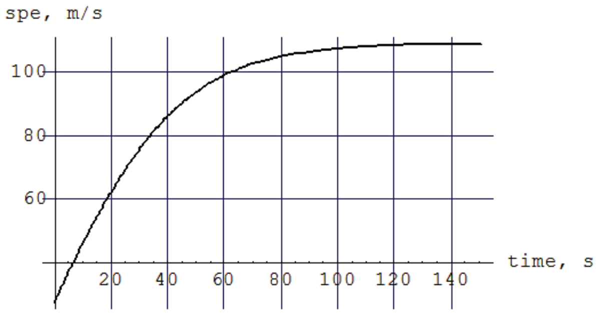

Fig. 3. The train's speed graph

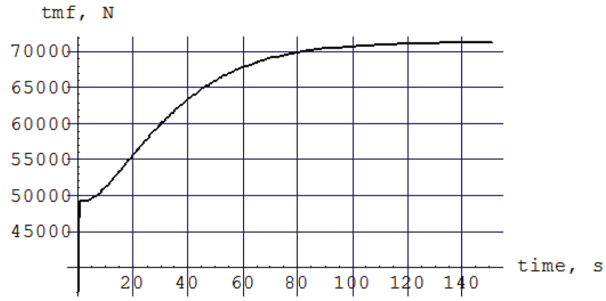

Fig. 4. The LSM's traction force graph

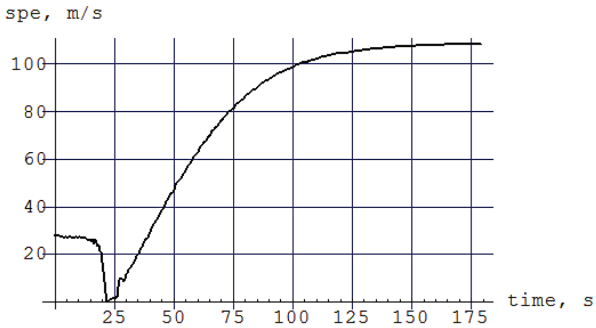

Fig. 5. The train's speed graph

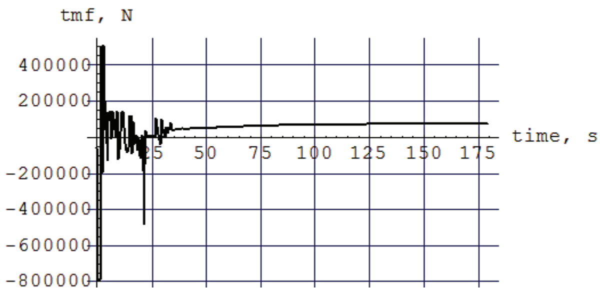

Fig. 6. The LSM's traction force graph

control; Fig. 5 and 6 – phase-frequency control; Fig. 1, 3, 5 show the train speed graphs; Fig. 2, 4, 6 – graphs of the LSD's traction force acting on it.

Analysis of the results of modeling the increase in train speed shows that it is unacceptable as an option to adjust only the frequency of the motor supply voltage – because of the high value of train acceleration, as well as the phase-frequency regulation of this voltage – because of the high-frequency oscillation of the MLT's speed. In addition, in the latter case, the LSM's armature's currents of are unacceptably high. The most suitable is the amplitude-frequency version of the armature's voltage control.

Train's entrance into the tunnel and the exit from it lead to differences in the aerodynamic resistance to motion by about 30% [13–15], which can lead to

Received: 11.08.2018. Revised: 11.08.2018. Accepted: 01.10.2018.
Transportation Systems and Technology. 2018;4(3):143-153

doi: 10.17816/transsyst201843143-153

sudden fluctuations in acceleration and speed of this motion. This is unacceptable and makes it expedient to automate the control by it. At the entrance and exit from the tunnel, additional resistance to motion changes almost linearly. Therefore, when modeling this mode of motion, it was considered that the aerodynamic resistance is described by the relations:

$$F^{*}_{ADx} = F_{ADx} \cdot [1 + (1/0.7 - 1) \cdot \kappa];$$

$$\kappa = \begin{cases} 0 & \forall\, x < \xi_{ts} - 0.5 \cdot l_t \vee x > \xi_{tf} + 0.5 \cdot l_t; \\ (x + 0.5 \cdot l_t - \xi_{ts}) \cdot l_t^{(-1)} & \forall\, \xi_{ts} - 0.5 \cdot l_t \le x \le \xi_{ts} + 0.5 \cdot l_t; \\ 1 & \forall\, \xi_{ts} + 0.5 \cdot l_t < x < \xi_{tf} - 0.5 \cdot l_t; \\ (\xi_{tf} - x + 0.5 \cdot l_t) \cdot l_t^{(-1)} & \forall\, \xi_{tf} - 0.5 \cdot l_t \le x \le \xi_{tf} + 0.5 \cdot l_t, \end{cases} \tag{9}$$

where l_t – the length of the train; ξ_{ts}, ξ_{tf} – the distances from the starting point of the way to the beginning and end of the tunnel. The aim of motion control in the tunnel:

$$\ddot{x}(t) = \ddot{x}_{ts} = const, \tag{10}$$

where $\ddot{x}_{ts}$ – acceleration of the train at the tunnel's entrance. Compliance with this condition is achieved by frequency, amplitude-frequency, or phase-frequency voltage U_a control. The required for this purpose laws of its change were found using the model (2) (in which F_{ADx} was replaced by a quantity F^{*}_{ADx}, that was calculated according to relations (9), and $\ddot{x}$ was replaced by a quantity $\ddot{x}_{ts}$, that was calculated according to (10)), as well as the LSM's dynamics model [2].

Illustrative examples of the results of the investigation of the MLT's motion in a tunnel are shown in Fig. 7–12. Fig. 7 and 8 correspond to controlling only the frequency of the armature voltage, Fig. 9 and 10 – amplitude-frequency control of this voltage, and Fig. 11 and 12 – phase-frequency control. Fig. 7, 9 and 11 show the train speed graphs, and in Fig. 8, 10 and 12 – graphs of the LSD's traction force acting on it.

Analysis of the simulation results of these three options of controlling the motion of the train through the tunnel leads to the following conclusions. In the case of only frequency control by supply voltage, the jump of the MLT's speed is about 10 %, which is definitely unacceptable. Other two methods of automatic voltage control are approximately equivalent, since in both of these cases there are no significant fluctuations of the MLT's speed and acceleration when passing the

Received: 11.08.2018. Revised: 11.08.2018. Accepted: 01.10.2018.

doi: 10.17816/transsyst201843143-153

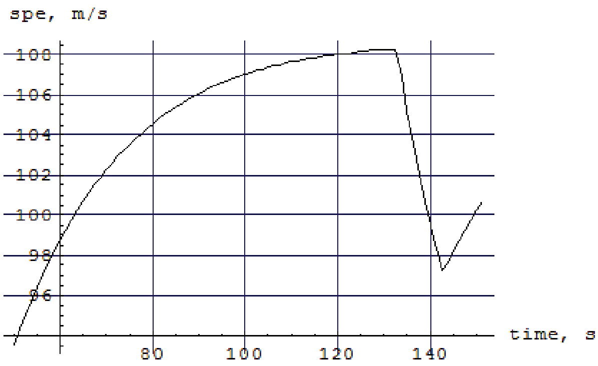

Fig. 7. The train's speed graph

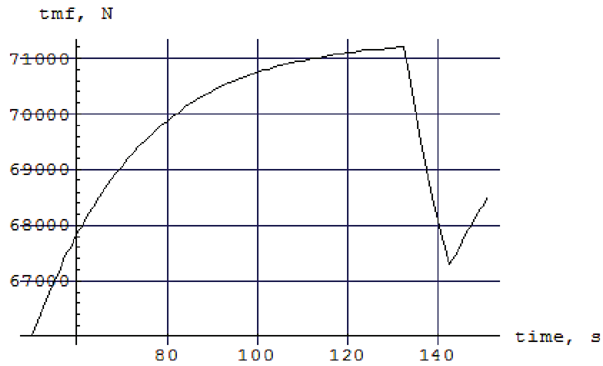

Fig. 8. The LSM's traction force graph

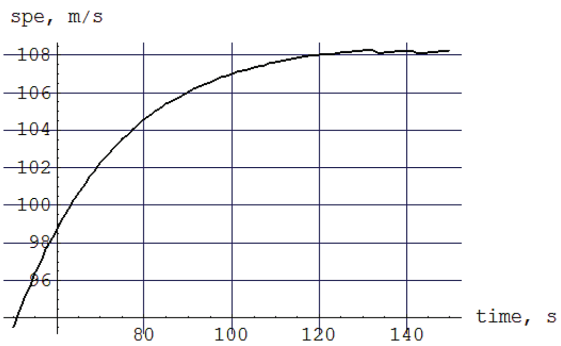

Fig. 9. The train's speed graph

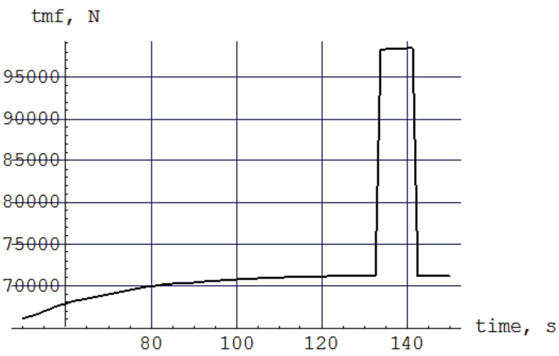

Fig. 10. The LSM's traction force graph

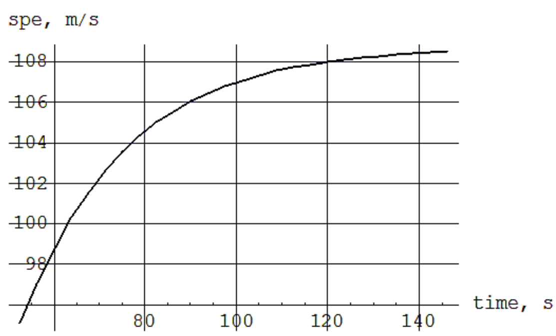

Fig. 11. The train's speed graph

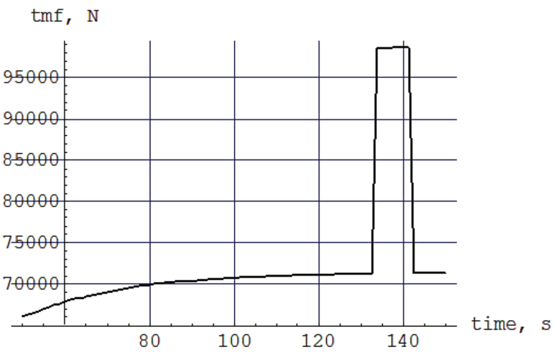

Fig. 12. The LSM's traction force graph

tunnel. At the same time, the phase-frequency control method is simpler (since there is no need to regulate high voltages). However, with amplitude-frequency control, the peak values of the phase currents are approximately one and a half times lower, which reduces the current load on the electrical equipment of the motor.

During the MLT's motion, the LSM's armature and inductor windings are reciprocally moved. In these windings, electromotive forces of mutual induction are induced, leading to the appearance of mechanical forces, which counteract the mutual displacement of the windings. The voltage feeding the armature winding of

Received: 11.08.2018. Revised: 11.08.2018. Accepted: 01.10.2018.
Transportation Systems and Technology. 2018;4(3):143-153

doi: 10.17816/transsyst201843143-153

the motor usually compensates of these electromotive forces and LSM operates in traction mode. But if the current value of the armature voltage decreases, the motor automatically goes into braking mode. As well as MLT's acceleration, its electrodynamics' breaking should be smooth. Therefore, the two most appropriate ways to implement service braking of the train are the amplitude-frequency and phase-frequency control of the LSM's armature voltage. To implement these smooth control modes, the amplitude and the initial phase of the armature voltage can vary, for example, according to the laws.

$$U_a(t) = U_a^* \cdot [1 - th(t \cdot k_{vi})]; \tag{11}$$

$$\theta_u(t) = -\alpha_u \cdot th(t \cdot k_{fm}), \tag{12}$$

where k_{vi}, k_{fm} – the coefficients determining the rate of amplitude and the initial phase of the armature voltage changing. These laws can be used for implementation of the train's service braking. For emergency braking, instantaneous removal of the supply voltage from the motor's armature winding is possible, but with the preservation of its circuits retained – by means of the double-breasted three-phase short circuit of this winding.

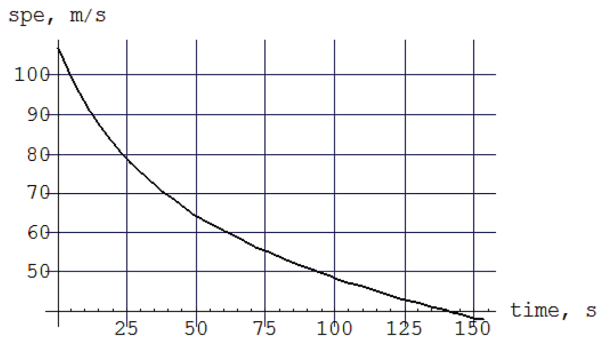

Fig. 13 The train's speed graph

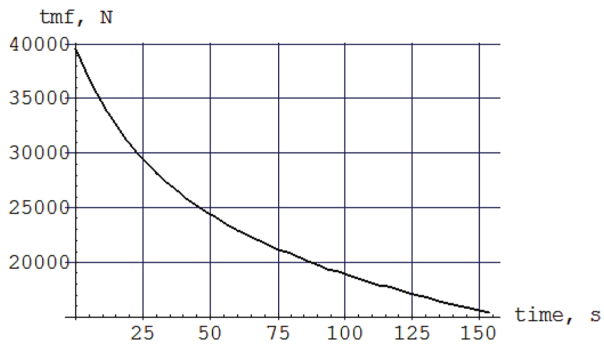

Fig. 14 The LSM's braking force graph

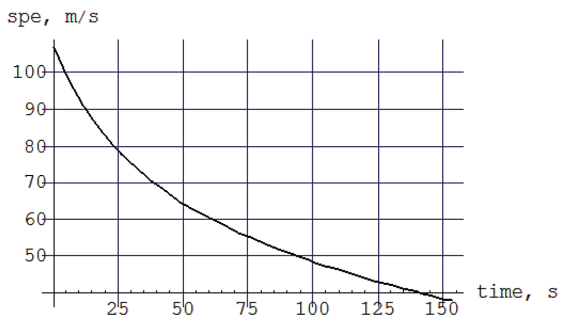

Fig. 15 The train's speed graph

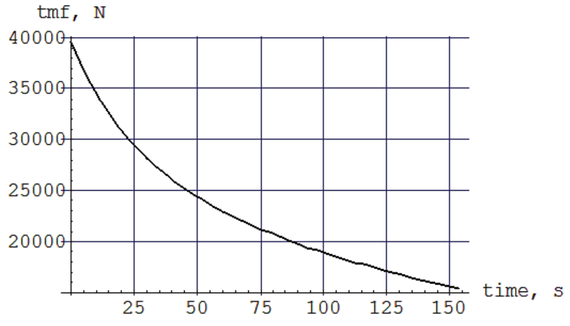

Fig. 16 The LSM's braking force graph

Received: 11.08.2018. Revised: 11.08.2018. Accepted: 01.10.2018.
Transportation Systems and Technology. 2018;4(3):143-153

doi: 10.17816/transsyst201843143-153

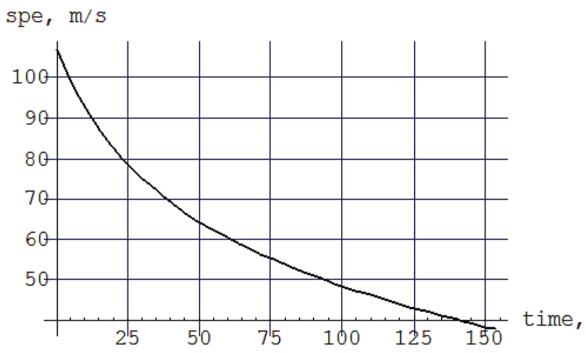

Fig. 17 The train's speed graph

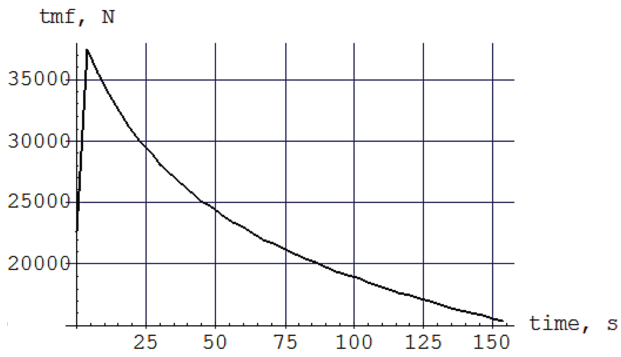

Fig. 18 The LSM's braking force graph

Illustrative examples of the investigation results of the MLT's motion in various braking regimes are shown in Fig. 13–18. Fig. 13, 14 correspond to the implementation of service braking with amplitude-frequency voltage control; Fig. 15, 16 – with phase-frequency control. Finally, Fig. 17, 18 correspond to emergency braking – by means of a double-breasted three-phase short circuit of the LSM's armature winding. Fig. 13, 15, 17 show graphs of train's speed; Fig. 14, 16, 18 – graphs of the LSM's braking force acting on it.

Analysis of the simulation results of the indicated MLT's motion brake regimes allows drawing the following conclusions. The considered modes of service braking (with amplitude-frequency and phase-frequency regulation of the motor's armature voltage) are approximately equivalent on the brake characteristics being realized. Both of them provide sufficient smoothness of the change in acceleration and speed of the train. The peak values of acceleration do not exceed $0.15 \cdot g$, which is quite acceptable. The implementation of emergency braking leads to significant peak acceleration – about $0.22 \cdot g$, which can't be eliminated. However, such a short-term increase in acceleration in extreme situations is justified.

CONCLUSIONS

By way of computer simulation, the dynamics of a magnetically levitated train, subjected to natural disturbances, and controlled by a linear synchronous motor, in the modes of acceleration, passage of the tunnel, as well as service and emergency braking are studied. The analysis of the obtained results made it possible to evaluate the dynamic qualities of the train in the considered non-stationary modes of motion, as well as its loading in their process. This solves the problem of this part of the study.

Received: 11.08.2018. Revised: 11.08.2018. Accepted: 01.10.2018.
Transportation Systems and Technology. 2018;4(3):143-153

doi: 10.17816/transsyst201843143-153

Библиографический список / References

1. Дзензерский В. А., Омельяненко В. И., Васильев С. В. и др. Высокоскоростной магнитный транспорт с электродинамической левитацией. – Киев: Наукова думка, 2001. – 479 с. [Dzenzerskii VA, Omel'yanenko VI, Vasil'ev SV, et al. Vysokoskorostnoi magnitnyi transport s elektrodinamicheskoi levitatsiei. Kiev: Naukova dumka; 2001. 479 p. (In Russ.)].
2. Atherton DL, Eastham AR. High speed Maglev studies in Canada. In: *5-Th International Cryogenic Engineering Conference (ICEC-5)*. Kyoto; 1974:46-50.
3. Zhigang L, Long Z. *Maglev Trains. Key Underlying Technologies*. Berlin: Springer, 2015:215.
4. Поляков В. А., Хачапуридзе Н. М. Модель процесса реализации тяговой силы двигателя магнитолевитирующего поезда//Наука та прогрес транспорту. Вісник Дніпропетровського національного університету залізничного транспорту ім. акад. В. Лазаряна – 2016. – № 4 (64). – С. 55–62. [Polyakov VA, Khachapuridze NM. Implementation Model of Motor traction Force of Maglev Train. *Science and Transport Progress. Bulletin of Dnipropetrovsk national university of railway transport named after academician V. Lazaryan* 2016;4(64):55-62. (In Russ.)]. doi: 10.15802/stp2016/77909
5. Fujiwara S. Superconducting Maglev and its electromagnetic Characteristics *SAE Technical Paper Series*. 1995;SAE 95-1922:1-6.
6. Lee KB, Kim CA. Study on Energy Efficiency Analysis by Maglev Trains. *Electrical and Electronic Engineering. Advanced Science and Technology Letters*. 2015;118:48-53.
7. Лебедев А. А. Динамика полёта беспилотных летательных аппаратов. – М.: Машиностроение, 1973. – 616 с. [Lebedev AA. *Dynamics of Flight of Unmanned Aerial Vehicles.* Moscow: Mashinodstroenie; 1973. 616 p. (In Russ.)].
8. Wairagade AKR, Balapure MBH, Ganer P. Magnetic Levitation Train. *Journal for Research.* 2015;01(08):1-5.
9. Chong Y, Kane W. Maglev train's development prospects in China *Maglev Train in China Journal.* 2016;2:75-90.
10. Дзензерский В. А., Зевин А. А., Филоненко Л. А. Устойчивость вертикальных колебаний в системе электродинамического подвеса с дискретной путевой структурой // Прикладная механика. – 1995 – Т. XXXI. – № 7. – С. 88–93. [Dzenzerskij VA, Zevin AA, Filonenko LA. Stability of vertical oscillations in a system of electrodynamic suspension with a discrete track structure *Applied Mechanics.* 1995; XXI(7):88-93. (In Russ.)].
11. Russell J, Cohn R. *List of Maglev Train*. Johannesburg: Book on demand; 2015. 135 p.
12. Antlauf W, Coates KC. Fast Tracks: Building the Shanghai Maglev *Civil Engineering.* 2004;11:59-66.
13. Fuji J. Ground transportation on suspension on superconducting magnets. II. Suspension system on superconducting magnets. *Dengakushi.* 1991;3:457-459. (In Japan).
14. Zhigang L, Zhiqiang L, Xiaolong L. *Maglev Trains*. Berlin: Springer; 2015. 250 p.
15. Tandan GK, Sen PK, Sahu G, et al. Review on Development and Analysis of Maglev Train *International Journal of Research in Advent Technology*. 2015;3(12):14-17.

Information about the authors:
Vladislav Polyakov, Ph. D. of Engineering Sciences;
eLibrary SPIN: 5744-2789; ORCID 0000-0002-4957-8028;
E-mail: p_v_a_725@mail.ru

Received: 11.08.2018. Revised: 11.08.2018. Accepted: 01.10.2018.

Nikolai Khachapuridze, Ph. D. of Engineering Sciences;
eLibrary SPIN: 2115-4942; ORCID 0000-0003-0682-6068;
E-mail: itst@westa-inter.com

Сведения об авторах:

Поляков Владислав Александрович, кандидат технических наук, старший научный сотрудник;
eLibrary SPIN: 5744-2789; ORCID 0000-0002-4957-8028;
E-mail: p_v_a_725@mail.ru

Хачпуридзе Николай Михайлович, кандидат технических наук, старший научный сотрудник;
eLibrary SPIN: 2115-4942; ORCID 0000-0003-0682-6068;
E-mail: itst@westa-inter.com

To cite this article:

Polyakov VA, Khachapuridze NM. Magnetically levitated train's longitudinal motion (simulation results). *Transportation Systems and Technology.* 2018;4(3):143–153. doi: 10.17816/transsyst201843143-153

Цитировать:

Поляков В. А., Хачапуридзе Н. М. Продольное движение магнитолевитирующего поезда (результаты моделирования) // Транспортные системы и технологии. – 2018. – Т. 4. – № 3. – С. 143–153. doi: 10.17816/tanssyst201843143-153